

A Consolidated Multi-rate Burst-Mode DPSK Transmitter Using a Single Mach-Zehnder Modulator

J. P. Wang, R. J. Magliocco, N. W. Spellmeyer, H. Rao, R. Kochhar, D. O. Caplan, and S. A. Hamilton[§]

MIT Lincoln Laboratory, 244 Wood St., Lexington, MA 02420, USA

jpwang@ll.mit.edu

Abstract: We demonstrate phase modulation, pulse carving, and burst-mode windowing in a single Mach-Zehnder modulator, significantly reducing size, weight, power, and complexity of prior three-modulator designs with only 0.6-dB additional performance penalty.

OCIS codes: (060.5060) Phase modulation; (060.2605) Free-space optical comm.; (060.4510) Optical communications

1. Introduction

High-sensitivity multi-rate optical transceivers are attractive for use in power-starved free-space communication applications such as NASA's deep-space networks [1, 2] since they enable operation over a variety of different links. Under challenging link conditions these transceivers provide fall-back modes to maintain bit-error-rate (BER) performance and under more favorable link conditions they can support high-throughput bandwidth-on-demand.

Recently, we demonstrated multi-rate optical differential phase-shift-keying (DPSK) using variable-duty-cycle burst-mode operation with near-theoretical receiver performance over a wide dynamic range of data rates (from Mb/s to Gb/s) [3]. The burst-mode DPSK waveform reduces the data rate by increasing the burst "off time" while maintaining a fixed slot rate, enabling a simple receiver design using a single commercially-available delay-line interferometer to demodulate lower data rates without penalty. In that previous work, the burst-mode transmitter waveforms were generated by a cascade of three Mach-Zehnder modulators (MZMs): a pulse carver to generate the return-to-zero (RZ) pulses, a data modulator which imparts the differential phase encoding, and a burst window modulator to extinguish the pulses during the "off time". While use of discrete modulators in this manner is a straightforward means of implementing these functions with good fidelity [4-7], this comes at the expense of increased size, weight, power (SWAP), and complexity by requiring three modulators and bias controllers as well as introducing excessive insertion loss in the transmitter. Since low-SWAP and simplicity are often important design drivers in free-space optical systems, a less-complex single-modulator solution is desirable.

Previous investigations into single-modulator DPSK transmitter designs have focused on non-burst-mode 10-Gb/s carrier-suppressed (CS) RZ-DPSK and RZ-DPSK for fiber transmission [8-10]. Our approach is similar to that of [9] where an RZ three-state electrical drive waveform is generated from complementary non-return-to-zero (NRZ) waveforms. In this work, we also incorporate burst-mode functionality with a single MZM which enables a consolidated multi-rate burst-mode DPSK transmitter implementation. Compared with the three-modulator transmitter, this consolidated design significantly reduces SWAP and complexity at a cost of ~0.6 dB additional receiver power penalty.

2. Background and Experimental Design

As noted above, burst-mode DPSK achieves multi-rate operation by increasing the "off time" between bursts of data while maintaining a fixed slot rate (Fig. 1a). To generate this waveform using a single modulator, we create a three-state electrical drive waveform (Fig. 1b) from DPSK-encoded data. A "+1" pulse indicates the presence of an optical pulse with a π phase. A "-1" pulse indicates the presence of an optical pulse with 0 phase. A "0" indicates the absence of an optical pulse. When this electrical waveform is used to drive a MZM biased at a transmission null, the resulting optical pulse train is a RZ DPSK-encoded waveform with "on" and "off" times as determined by the electrical drive encoding. The input three-state electrical drive, scaled to $2V_{\pi}$, is shown relative to the transfer function of a lithium-niobate MZM. The resulting optical output waveform is shown on the right in blue.

To generate the three-state electrical drive waveform, we first separately generate the positive ("+1") and negative ("-1") pulses and then linearly sum the results. The positive pulses (D1) are generated by $D1 = B \text{ AND } P$, where B is the burst window information and P is the DPSK-encoded data. The negative (D2) pulses are generated using $B \text{ AND } (P \text{ XOR } B)$. The result (Fig. 1c) is that D1 is high (V_h) when there is a pulse of π phase, and D2 is high (V_h) when there is a pulse of 0 phase. We then take the complement of D2, which is low (0) when there is a pulse of 0 phase. The electrical sum of D1 with the complement of D2 results in a three-state waveform which has a value of $2V_h$ when there is a pulse of π phase (both D1 and the complement of D2 are high), V_h when there is no pulse (D1 is 0 and the complement of D2 is high) and 0 when there is a pulse of 0 phase (D1 is 0 and the

[§] This work was sponsored by the Department of the Air Force under Air Force Contract #FA8721-05-C-0002. Opinions, interpretations, conclusions, and recommendations are those of the author and are not necessarily endorsed by the United States Government.

OWX3.pdf

complement of D2 is low). The modulator is biased at null to obtain the correct DPSK-encoded burst data, enabling simple bias control compared with the three-modulator design, which requires three bias control loops: one to bias the pulse carver at quadrature, one to bias the data modulator at a null, and a more complex bias control loop to correctly bias the burst modulator given the variable duty cycle burst window waveforms.

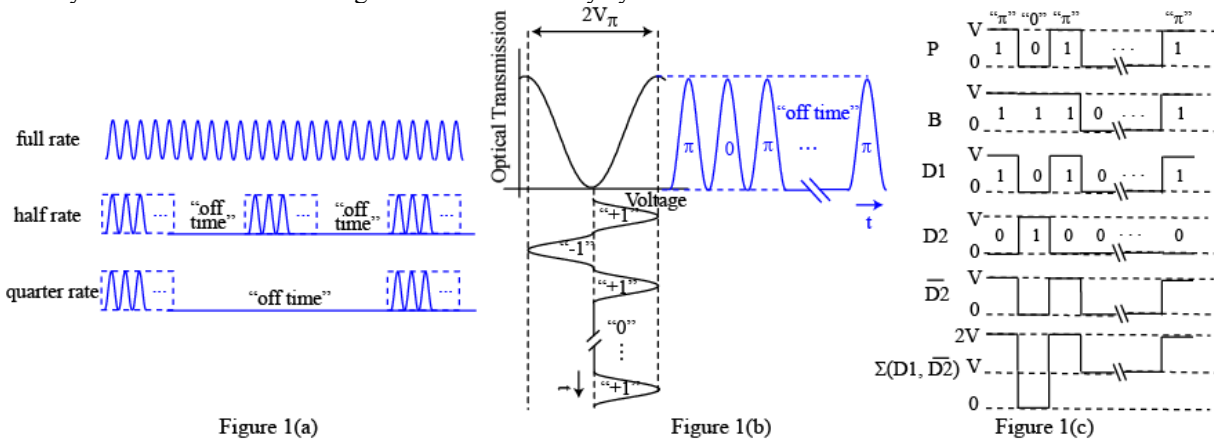


Figure 1: (a) Example of burst-mode waveforms indicating the increase in "off time" for lower data rates. (b) MZM optical transfer function showing how the three-state electrical drive results in a DPSK-encoded RZ burst-mode optical output. (c) Process for generating the three-state electrical waveform beginning with the DPSK-encoded phase (P) and the burst window (B). D1 represents the positive pulses while D2 represents the negative pulses.

The consolidated multi-rate RZ DPSK transmitter design is shown in Fig. 2. A Xilinx Virtex-5 field programmable gate array (FPGA) generates the logical signals D1 and D2. Each FPGA output signal is retimed with a latched comparator to avoid runt pulses and converted from NRZ to RZ by an Inphi chip (13706RZ). Time-aligned RZ-D1 and RZ-D2 pulses are combined, amplified, and filtered to provide the required drive waveform and pulse shaping in the modulator. The inset in Fig. 2 shows the electrical drive waveform after electrical summation. The system operates at 3.375 GHz, which when combined with a Reed-Solomon (255, 191) code results in a maximum data rate of 2.5 Gb/s.

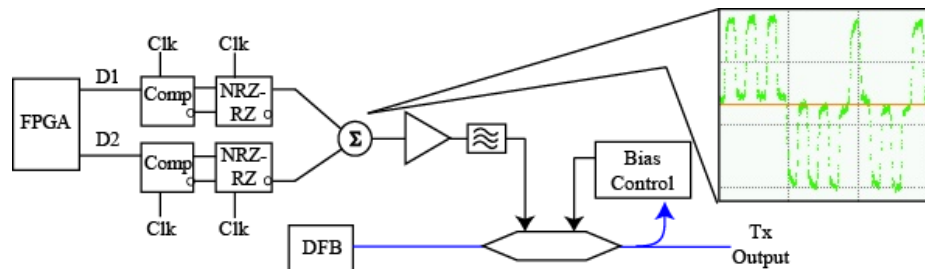


Figure 2: Experimental schematic. The FPGA performs DPSK encoding and generates the three-state waveforms D1 and D2. A latched comparator (Comp) is used to retime the FPGA output, followed by the NRZ to RZ converter. Both devices are driven by a 3.375 GHz clock. The sum is performed with a resistive power combiner preceded by 6-dB pads to reject reflections. The gain stage is a high linearity traveling-wave amplifier needed to drive the modulator to $2V_\pi$, followed by a 5 GHz filter for pulse shaping. The DFB laser outputs 1558.9 nm. The electro-optic modulator has a V_π of 3.2V and 31-dB extinction at DC. Inset shows electrical drive waveform prior to amplification and filtering.

An important aspect of the electrical drive is the linearity of the amplifier required to drive the electro-optic modulator. This amplifier should contribute minimal jitter and exhibit flat group delay over the operating range while providing sufficient gain to drive the modulator to $2V_\pi$. We selected a multi-stage traveling-wave amplifier (Centellax) biased for optimal performance to meet these requirements. To ensure proper timing between the RZ-D1 and RZ-D2 pulses, we used phase-matched coaxial cables for data and RF phase shifters for the clock distribution. A 5-GHz low-pass filter after the RF amplifier provided RZ pulse shaping matched to our receiver design. We used a 3.2V V_π electro-optic modulator with ~ 30 -dB-class extinction at DC. As described in our previous work [3], a burst modulator extinction of 30 dB enables <0.5 dB additional penalty down to 20 Mb/s.

3. Results

To evaluate the multi-rate performance of the consolidated single-modulator transmitter, we compared the BER penalty with that of the three-modulator transmitter. We used an unpolarized, pre-amplified DPSK receiver with

balanced photodetectors and matched filtering similar to that described in [3]. We used a Reed-Solomon (255,191) encoded $2^{31}-1$ pseudo-random bit sequence (PRBS) and measured performance from 13.1 Mb/s to 2.5 Gb/s. As shown in Fig. 3, we demonstrated performance at 2.7 dB from theory, indicating an additional penalty of 0.6 dB over the three-modulator design. This difference is largely a result of the additional bandwidth of RZ data modulation resulting in increased pattern dependence. At low data rates (≤ 52 Mb/s), the consolidated transmitter performance was only limited by the modulator extinction ratio [11]. We obtained a good fit (Fig 3, inset) to the measured penalty with a modulator extinction ratio of 28 dB.

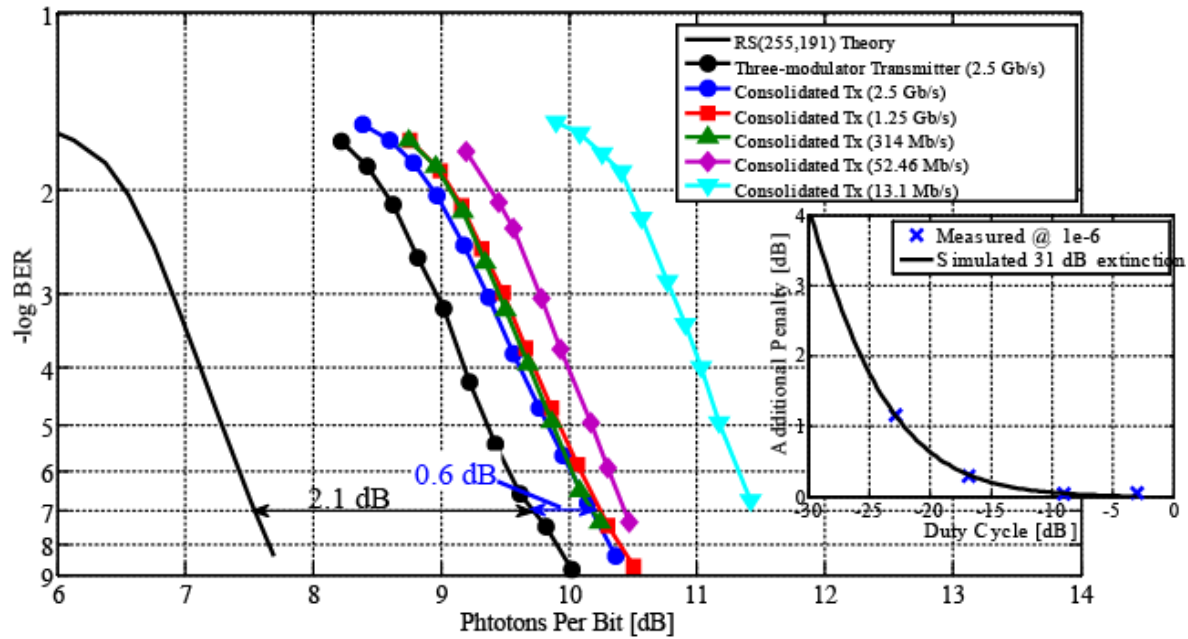


Figure 3: Multi-rate consolidated DPSK transmitter performance for a $2^{31}-1$ PRBS from 13.1 Mb/s to 2.5 Gb/s, compared with the three-modulator transmitter performance at 2.5 Gb/s. Inset shows a good fit of the measured penalty to a 28-dB extinction ratio modulator.

4. Conclusions

In summary, we have demonstrated a consolidated multi-rate burst-mode DPSK transmitter which implements phase modulation, pulse carving, and burst-mode windowing in a single Mach-Zehnder modulator. This significantly reduces size, weight, power, and complexity of prior three-modulator designs with only 0.6-dB additional performance penalty.

4. References

- [1] C. D. Edwards, *et al.*, "NASA Deep Space Telecommunications Road Map," in *Telecommunications and Mission Operations Progress Report 42-136, Jet Propulsion Laboratory*, 1999.
- [2] S. A. Townes, *et al.*, "The Mars laser communication demonstration," in *IEEE Aerospace Conf.*, 2004.
- [3] D. O. Caplan, *et al.*, "Ultra-wide-range Multi-rate DPSK Laser Communications," in *CLEO*, Paper CPDA8, 2010.
- [4] A. H. Gnauck, *et al.*, "Demonstration of 42.7-Gb/s DPSK receiver with 45 photons/bit sensitivity," *IEEE Photon. Technol. Lett.*, vol. 15, pp. 99-101, Jan 2003.
- [5] J. H. Sinsky, *et al.*, "RZ-DPSK Transmission Using a 42.7-Gb/s Integrated Balanced Optical Front End With Record Sensitivity," *J. Lightwave Tech.*, vol. 22, Jan. 2004.
- [6] N. W. Spellmeyer, *et al.*, "High-sensitivity 40-Gb/s RZ-DPSK with forward error correction," *IEEE Photon. Technol. Lett.*, vol. 16, pp. 1579-1581, June 2004.
- [7] D. O. Caplan, *et al.*, "Demonstration of Optical DPSK Communication with 25 Photons/Bit Sensitivity," in *CLEO*, 2006.
- [8] Y. J. Wen, *et al.*, "RZ/CSRZ-DPSK and Chirped NRZ Signal Generation Using a Single-Stage Dual-Electrode Mach Zehnder Modulator," *IEEE Photon. Technol. Lett.*, vol. 16, 2004.
- [9] X. Liu, *et al.*, "Chirped RZ-DPSK Based on Single Mach-Zehnder Modulator and Its Nonlinear Transmission," *IEEE Photon. Technol. Lett.*, vol. 17, 2005.
- [10] Y. Dong, *et al.*, "RZ/CSRZ-DPSK signal generation using only one Mach-Zehnder modulator," in *OFC*, 2006.
- [11] D. O. Caplan, "Laser communication transmitter and receiver design," *J. Opt. Fiber Commun. Res.*, vol. 4, pp 225-362, 2007.